Food & Function

ROYAL SOCIETY OF CHEMISTRY

PAPER

View Article Online
View Journal | View Issue

Cite this: *Food Funct.*, 2025, **16**, 3508

Sodium butyrate attenuates experimental neonatal necrotizing enterocolitis by suppressing TLR4-mediated NLRP3 inflammasome-dependent pyroptosis†

Yanan Gao,‡[a] Liting Yang,‡[a,b] Hongya Wu,[a] Qianqian Yao,[a,c] Jiaqi Wang[a] and Nan Zheng *[a]

Necrotizing enterocolitis (NEC) is a fatal intestinal disease in premature infants, and is characterized by intestinal inflammation and disruption of the intestinal barrier. The protective effects of sodium butyrate (NaB) against NEC have been documented, however, the underlying fundamental processes remain unknown. To address this deficit, we used the NEC neonatal rat model to confirm the intestinal protective effect of NaB. We then used network pharmacology and confirmed a role for NaB in the attenuation of NEC and this was associated with the NLRP3 inflammasome and the NF-κB signaling pathway. These results were verified by proteome analysis *in vivo*, and molecular docking analysis was used to explore the potential underlying mechanisms, revealing a suppressive function of NaB on NEC, which may be caused by its interaction with the TLR4-mediated NF-κB signaling pathway. An *in vitro* cell model (LPS-stimulated IEC-6 cells) was then established to confirm the docking results. Results using assays involving the NLRP3 (MCC950) and TLR4 (TAK-242) inhibitors suggested that NaB protected intestinal cells from inflammatory injuries during NEC by suppressing the TLR4/MyD88/NF-κB/NLRP3/cleaved caspase-1/GSDMD inflammasome pathway. These findings indicated that NaB can be used as a potential modulatory and therapeutic candidate for the treatment of NEC.

Received 23rd July 2024,
Accepted 9th January 2025

DOI: 10.1039/d4fo03517h

rsc.li/food-function

1. Introduction

Necrotizing enterocolitis (NEC) is a fatal inflammatory intestinal disease found in preterm infants, and is considered as the first cause of short bowel syndrome in neonates.[1] NEC manifests as necrosis of the intestinal mucosa and even the distal ileum and proximal colon, with a mortality rate as high as 30%.[2] Besides the intestinal inflammation, the clinical manifestations of NEC are often accompanied by intestinal barrier dysfunction. Intestinal epithelial apoptosis and autophagy are up-regulated in Sprague–Dawley (SD) neonatal rats with NEC.[3,4] Additionally, the expression of tight junction (TJ) proteins was down-regulated in rat pups with NEC.[5] Compared to the healthy gut, the intestinal tissue of NEC patients showed a greater loss of villus structure, with more severe submucosal damage (partial necrosis) and increased inflammatory cell infiltration.[6] Moreover, NEC may be related to long-term complications, including neurodevelopmental impairment, cognitive alterations, and multisystem organ failure.[7] Consequently, it is essential to develop innovative strategies for the prevention or treatment of NEC.

Comprehensive data from *in vitro*, *in vivo*, and human cohort studies have shown that breast milk helps lower the prevalence of NEC by 6- to 10-fold.[8] A previous review reported that feeding preterm infants with breast milk and probiotics could effectively inhibit the frequency of NEC, which could not be achieved by infant formula and probiotics.[9] The primary difference between these two combinations is that breast milk with probiotics could produce additional metabolites, including indole-3-lactic acid and short-chain fatty acids (SCFAs).[10] In another study, various SCFAs, including butyrate, acetate, and formate, have been found to exist in breast milk samples at concentrations of 95.6, 46.8, and 43.7 μmol L^{-1}, respectively.[11] In addition, butyrate has also been found in the milk of various other mammals, including cow, buffalo, goat, yak, and camel.[12] Another study reported the presence of butyrate

[a]*Institute of Animal Sciences, Chinese Academy of Agricultural Sciences, Beijing 100193, China. E-mail: zhengnan@caas.cn; Tel: +86-10-62816069*
[b]*Institute of Food Science and Technology, Chinese Academy of Agricultural Sciences, Beijing 100193, China*
[c]*Department of Food Science, Faculty of Veterinary Medicine, University of Liège, Liège, Belgium*

†Electronic supplementary information (ESI) available. See DOI: https://doi.org/10.1039/d4fo03517h

‡These authors contributed equally to this work.

in different heat-treated milk samples.[13] Butyrate is not only the most abundant SCFA in breast milk but also the focus of attention in studies focusing on SCFAs that regulate intestinal health.

Due to the double-sided effect of butyrate on intestinal health and the limited studies focusing on the effects of sodium butyrate (NaB) on NEC, only a few studies have reported the protective effect of butyrate on the intestine of NEC patients. A previous study of 81 NEC patients showed that butyrate levels in the fecal samples of NEC patients were lower than controls.[14] Examination of the C57BL/6 mice administered with NaB showed that NaB exerted protective effects in the disrupted intestine of this NEC model by downregulating inflammatory cytokines (IL-6 and TNF-α) and upregulating a TJ protein (claudin-7).[15] In addition, our previous *in vitro* and *ex vivo* studies showed that NaB exhibited anti-inflammatory effects in the lipopolysaccharide (LPS)-induced neonatal NEC intestine.[16,17] However, it is still unknown whether NaB can exert intestinal protective effects in an *in vivo* NEC model. Moreover, the potential mechanisms underlying the therapeutic or preventive effects of NaB on NEC patients are also unknown.

Human development studies have shown that newborn rat pups are an excellent model to study preterm neonates.[18] Furthermore, based on public databases, network pharmacology has been regarded as an emerging, high throughput, and cost-effective approach for identifying the potential targets of various compounds and diseases.[19] Proteomics provides a global perspective on the cellular processes of health and disease at the protein level.

In this study, the protective effect of NaB against NEC was confirmed in a neonatal rat model of NEC. The combination of proteomic experiments *in vivo* and network pharmacology was applied to explore the underlying potential core targets and pathways. Then, the potential underlying mechanisms were preliminarily validated by molecular docking analysis, and then the therapeutic role of NaB was experimentally verified using IEC-6 cells induced with LPS and inhibitor assays. These findings extend the nutritional function of NaB, which could be considered as a novel preventive and therapeutic agent for NEC.

2. Materials and methods

2.1 Chemicals

NaB (99% purity) was purchased from Sigma Aldrich (Natick, MA, USA). The lipopolysaccharide (LPS, bs-8000P) from *Escherichia coli 055: B5* was purchased from Bioss Corporation (Beijing, China). The primary antibodies, including anti-MyD88 (cat. no. bs-1047R), anti-TLR4 (cat. no. bs-20594R), anti-cleaved caspase-1 (cat. no. bs-10743R), anti-β-actin (cat. no. bs-0061R), and secondary antibodies were obtained from Bioss (Beijing, China). Anti-NLRP3 (cat. no. A12694) and anti-GSDMD (cat. no. 17308) antibodies were purchased from Abclonal (Wuhan, China). Anti-NF-κB p65 (cat. no. 8242S) was purchased from Cell Signaling Technology (MA, USA). The NLRP3 inhibitor (cat. no. MCC950) and TLR4 inhibitor (cat. no. TAK-242) were purchased from MedChemExpress (New Jersey, USA) and Selleck (Houston, USA), respectively.

2.2 Experimental neonatal NEC model *in vivo*

2.2.1 Animal studies. Twenty-four 3-day-old neonatal Sprague-Dawley rat pups were obtained from Wuhan Cloud Clone Diagnostic Reagent Institute Co., Ltd, (Wuhan, China) and divided into the control group (n = 8, fed with breastmilk freely), the NEC group (n = 8, fed with rodent formula, and administered with phosphate-buffered saline post-NEC modeling for 18 days *via* gavage administration at a dose of 0.1 mL day^{-1}), and the NEC + butyrate group (n = 8, fed with rodent formula, and administered with 14 mg per kg body weight NaB post-NEC modeling for 18 days by gavage administration at a dose of 0.1 mL day^{-1}). The experimental *in vivo* neonatal NEC model was established by hypoxia and cold stress, as described previously.[20] To improve the survival rate of the pups and simulate bowel necrosis histologically, we chose 3-day-old newborn SD rats instead of the rat pups after birth to establish the model. Briefly, the 3-day-old newborn SD rats were fed rodent formula (Abbott Nutrition, USA) and placed under an environment of 5% oxygen + 95% nitrogen for 10 min and then exposed to 4 °C for 10 min in a refrigerator. Hypoxia + cold stress stimulation was performed twice daily for three consecutive days. On the 4th day, the rats were sacrificed. A score of 0 to 4 was used to diagnose the severity of the NEC, as previously described and a score of ≥2 represents the occurrence of NEC.[20] The dosage of NaB in this study was selected based on previously reported studies.[15,21] Ileum tissue of these pups was obtained and stored at −80 °C for further experiments. The animal experiments were approved by the Committee for the Management and Use of Laboratory Animals [Review number: IACU21-0869 (Date: 7/2021)].

2.2.2 Reverse transcription-quantitative real-time polymerase chain reaction (RT-qPCR). We conducted RT-qPCR using the TB Green Premix Ex Taq II kit (Takara, Japan) following the manufacturer's protocol. First, total RNA was extracted from the ileum tissues of the neonatal SD rats using a TRIzol kit. Then, the extracted RNA was reverse transcribed into cDNA using the PrimeScript™ RT Reagent kit. The $2^{-\Delta\Delta Ct}$ method was used to calculate the changes in gene expressions levels relative to the GADPH expression as the reference gene. The primer sequences of the gene targets are shown in Table S1.†

2.2.3 Proteomics. Tandem mass tags (TMT)-based proteomic analysis was used to identify the pathways and proteins potentially involved in the protective action of NaB against NEC. Ileum tissues were vortexed and lysed in a lysis buffer and then subjected to protein digestion. One hundred micrograms of the collected protein was incubated, washed, and desalted. Then, the resultant labeled peptide was subjected to high pH reverse phase separation, followed by nano-HPLC-MS/MS analysis. Differentially expressed proteins (DEPs) were chosen based on two criteria: fold change >1.5 and $p < 0.05$. And then KEGG enrichment analysis was performed. The mass

spectrometry proteomics data have been deposited to the iProX (https://www.iprox.org) with the data set identifiers IPX0006818000.

2.2.4 Western blot assay. Ileum tissue samples were placed in RIPA lysate buffer for 30 min and then homogenized and centrifuged. Next, the supernatants, containing ileum proteins, were collected and denatured at 100 °C with a 5× protein loading buffer. After separation by SDS-PAGE, the membranes were blocked for 1.5 h. Then, the membranes were incubated overnight at 4 °C with primary antibodies, including anti-NLRP3, anti-GSDMD, anti-NF-κB p65, anti-TLR4, and anti-MyD88, at 1 : 1000, followed by incubation with secondary antibodies. The proteins were quantified using an enhanced chemiluminescence (ECL) kit, and the obtained band intensities were analyzed using Image J 2×.

2.3 Network pharmacology

2.3.1 Screening for potential targets of NaB and NEC. Bioinformatics analysis was used to screen the potential targets of small molecule (NaB) and NEC disease.

Potential targets for NaB in Homo sapiens were obtained from the Similarity ensemble approach (SEA, https://sea.bkslab.org), PharmMapper (https://lilab-ecust.cn/pharmmap), SuperPred (https://prediction.charite.de), and SwissTargetPrediction (https://www.swisstargetprediction.ch). The combined targets selected by these software were considered the potential targets of NaB.

Furthermore, the potential targets for NEC were summarized from DisGeNET (https://www.disgenet.org), GeneCards (https://www.genecards.org), MalaCards (https://www.malacards.org), and RGD Disease (https://rgd.mcw.edu/wg/portals/). These combined targets were considered as the potential targets for NEC.

2.3.2 Protein–protein interaction (PPI) network and enrichment analysis. STRING and Cytoscape software were used to construct the PPI network for NaB and NEC targets. Then, Cytoscape with the cytoHubba plug-in was used to build the PPI interaction network for "hub genes" for NaB and NEC. The cytoHubba plug-in ranks these "hub genes" according to their attributes of nodes in the network with 11 scoring methods. Among these scoring methods, the Maximal Clique Centrality (MCC) method was applied in the present study, as it has been reported to perform better than other scoring methods.[22] In addition, STRING (https://cn.string-db.org/) was also used to perform GO and KEGG pathway analysis enriched with hub genes. The selected visual enrichment of GO and KEGG analysis was conducted *via* GraphPad 9.00 and Origin 2021, based on a false discovery rate <0.05.

2.4 Molecular docking

Molecular docking between NaB and its targets was performed using the AutoDock software. The structure of NaB (ZINC895132) was obtained from the ZINC database (https://zinc15.docking.org), and the structure of their targets was searched from the PDB database (https://www.rcsb.org/).

2.5 LPS-induced *in vitro* experimental NEC model

2.5.1 Cell culture and treatments. Rat small intestinal epithelial cells (IEC-6, American Type Culture Collection, Manassas, VA, USA) were cultured in Dulbecco's modified Eagle's medium (DMEM) supplemented with 10% fetal bovine serum (FBS), 1% nonessential amino acids (NEAAs), and antibiotics. The culture was incubated in a 5% CO_2 incubator at 37 °C. DMEM, FBS, NEAAs and antibiotics were obtained from Gibco (Grand Island, NY, USA).

2.5.2 Cell viability and construction of *in vitro* experimental NEC model. The viability of IEC-6 cells was measured using a cell counting kit-8 assay according to the manufacturer's instructions. Cell viability (%) was presented as 100 times the ratio of the treatment group to the control group. According to previous studies, the *in vitro* NEC model using IEC-6 cells was established by exposing cells to different doses of LPS for different incubation times.[23–25] The *in vitro* NEC model was established by exposing IEC-6 cells to 100 μg mL^{-1} LPS for 3 h in the present study, which resulted in significantly decreased cell viability (Fig. S1†). The viability of IEC-6 cells induced by varying NaB concentrations (5–30 mM) for 2 h was measured. For subsequent analyses, IEC-6 cells pretreated with 5 mM NaB for 2 h and then 100 μg mL^{-1} LPS for 3 h were used (Fig. S2†).

2.5.3 RT-qPCR analysis and western blot assay. RT-qPCR was conducted as per the manufacturer's protocol. PrimeScript™ RT Reagent kit was used to reverse-transcribe the extracted RNA into cDNA. RT-qPCR was conducted using the TB Green Premix Ex Taq II kit (Takara, Japan) and GADPH was used as the reference gene. The $2^{-\Delta\Delta Ct}$ method was used to assess the relative expressions of genes. Among the primary antibodies, anti-NLRP3, anti-GSDMD, anti-NF-κB p65, anti-TLR4, anti-cleaved caspase-1, and anti-MyD88 were used for the western blot assay.

2.5.4 Determination of IL-1β and IL-18. The concentrations of IL-1β and IL-18 in the supernatant of the treated IEC-6 cells were determined with rat IL-1β (SEKR-0002) and rat IL-18 ELISA kits (SEKR-0054). These kits were obtained from Solarbio (Beijing, China).

2.5.5 TLR4 and NLRP3 inhibitor assay. NaB, TAK-242 (TLR4 inhibitor), or MCC950 (NLRP3 inhibitor) alone do not affect IEC-6 cell viability but can improve the viability of LPS-treated cells. In the present study, the pretreated IEC-6 cells were exposed to either 25 μM TAK-242 or 10 nM MCC950 (Fig. S3 and S4†).

For TAK-242-treated cells, the levels of TLR4, MyD88, NF-κB, NLRP3, cleaved caspase-1, and GSDMD proteins were measured. For MCC950-treated cells, the protein levels of NLRP3, cleaved caspase-1, and GSDMD and mRNA levels of *IL-1β*, *IL-4*, *IL-6*, *IL-18*, *TNF-α*, and *IFN-γ* were measured.

2.6 Statistical analyses

All the phenotypic data were analyzed using GraphPad Prism 9.0 (La Jolla, CA, USA) and the *in vivo* and *in vitro* results were represented as mean ± SEM. One-way ANOVA tests combined

with Tukey's multiple analysis was used to analyze differences and a $p < 0.05$ represented a significant difference.

3. Results

3.1 NaB ameliorated *in vivo* hypoxia- and cold stress-induced intestinal inflammation and disrupted intestinal barrier

To evaluate the protective effects of NaB on NEC-induced intestinal inflammation and disrupted intestinal barrier, *in vivo* experiments were conducted on neonatal rats with NEC (Fig. 1A). The results showed that NaB supplementation alleviated NEC-induced weight loss, especially on the seventh day ($p < 0.05$, Fig. 1B) and significantly reversed the NEC-induced changes in mRNA levels of proinflammatory cytokines ($p < 0.05$, Fig. 1C). These results indicated that NaB ameliorated NEC-induced intestinal inflammatory responses.

Additionally, the RT-qPCR results showed that NEC significantly reduced the mRNA levels of *claudin-3*, *claudin-7*, *occludin*, and *ZO-1* ($p < 0.05$, Fig. 1D), which represent the important markers of TJs. Furthermore, compared to the control group, the relative mRNA expression of cell apoptosis related genes (*Bax*, *Bcl-2*, *caspase-6*, and *caspase-9*) and cell autophagy related genes (*Atg5*, *Atg7*, *Atg12*, *ULK1*, *ULK2*, and *Beclin1*) were significantly increased in the NEC group ($p < 0.05$, Fig. 1E and F). However, gavage administration of 14 mg per kg b.w. NaB significantly reversed the changes in intestinal barrier-related (TJs, cell apoptosis and autophagy) mRNA levels induced by NEC ($p < 0.05$, Fig. 1D–F). These results showed that NaB had the ability to alleviate the disrupted intestinal barrier in neonatal rats with NEC.

3.2 Network pharmacology construction of NaB against NEC

To explore the underlying mechanisms of the protective effects of NaB against NEC, the network pharmacology was used in the present study.

3.2.1 Screening for potential NaB targets involved in the alleviation of NEC. There were 6, 50, 82, and 68 NaB targets for Homo sapiens in PharmMapper, SEA, SuperPred, and SwissTargetPrediction databases, respectively. After removing the duplicates, 199 NaB targets were collected (Fig. 2A). Using "necrotizing enterocolitis" as the keyword, 209, 463, 29, and 10 NEC targets in Homo sapiens were obtained from DisGeNET, GeneCards, MalaCards, and RGD Disease, respectively. After removing the duplicates, 577 NEC targets were collected (Fig. 2B) and used for subsequent analyses.

3.2.2 PPI network and enrichment analysis of hub genes. The PPI network of NaB and NEC targets was primitively constructed using the STRING database. To further visualize these constructed PPI networks, the data of both networks were imported into Cytoscape 3.9.1 to construct visual and analyzable PPI networks (Fig. 2C). The PPI network of NaB targets contained 147 nodes with 513 edges, and that of NEC targets comprised of 508 nodes with 12 776 edges. The nodes indicated the proteins, and the edges represented the interactions between the proteins. Next, the two networks were combined to obtain an overlapping PPI network between the NaB and NEC targets. This overlapping PPI network comprised 637 nodes and 13 264 edges. To further assess the hub genes in the overlapping PPI network, topology analysis was conducted using the cytoHubba plug-in of Cytoscape. Here, the top 50 targets, selected using the MCC scoring method in cytoHubba, were considered the hub genes. Table S2† shows detailed information on these top 50 hub genes. Finally, the PPI network of these hub genes comprised 50 nodes with 1193 edges and the degree values of these 50 hub genes were calculated. The target nodes with high degree values included NLRP3 ($n = 35$), CXCL1 ($n = 44$), CASP1 ($n = 46$), and MyD88 ($n = 46$), indicating that these might play an important role in the anti-NEC effects of NaB (Fig. 2D). In addition, the inflammation-related hub genes, including IL-18 ($n = 30$), IL-6 ($n = 20$), TLR4 ($n = 13$), and IL-1β ($n = 9$), were also found to be involved in the anti-NEC effects of NaB (Fig. S5†). These hub genes are primarily involved in the GO terms of the NLRP3 inflammasome complex (NLRP3 and CASP1) and the KEGG pathway of the NF-κB signaling pathway (IL-1β, CXCL8, TLR4, and MyD88, Fig. 2E and F). The detailed information for the enriched GO terms and KEGG pathways is depicted in Tables S3 and S4.†

3.3 Quantitative proteome analysis of the effects of NaB on neonatal rats with NEC

To verify the results obtained by the network pharmacology enrichment analysis suggesting that the NLRP3 inflammasome complex and the NF-κB signaling pathway might be the core anti-NEC targets of NaB, TMT proteomic analysis was conducted on the ileum of neonatal rats.

Firstly, the results of hierarchical clustering revealed that there are similarities in the expression patterns between NEC treatment and NEC + Butyrate treatment, while these two treatments were clearly separated from the control treatment (Fig. 3A). These results illustrated that NEC and NaB treatment led to all of the significant changes seen in the neonatal rats. This result was consistent with PCA analysis, which indicated that the NaB supplementation significantly impacted NEC progression (Fig. S6†). Additionally, as the histogram shows, there were 953 (432 up-regulated and 521 down-regulated), 513 (258 up-regulated and 255 down-regulated), and 65 (28 up-regulated and 37 down-regulated) DEPs in NEC *vs.* control, NEC + Butyrate *vs.* control, and NEC + Butyrate *vs.* NEC groups, respectively (Fig. 3B). These results suggested that NaB treatment could partly reverse the changes induced by NEC. The volcano diagram depicted the specific changes in DEPs among the different treatments (Fig. S7†).

To further elucidate the effects of NEC and NaB treatment on neonatal rats, KEGG pathway analysis was used to investigate intestinal inflammation- and intestinal barrier-related effects under different treatment conditions. The results of KEGG pathway enrichment showed that TJ, apoptosis and autophagy-related pathways were enriched by the DEPs (Fig. 3C–E). These results were consistent with the enrichment analysis of GO terms (Fig. S8†), suggesting that NaB attenuated

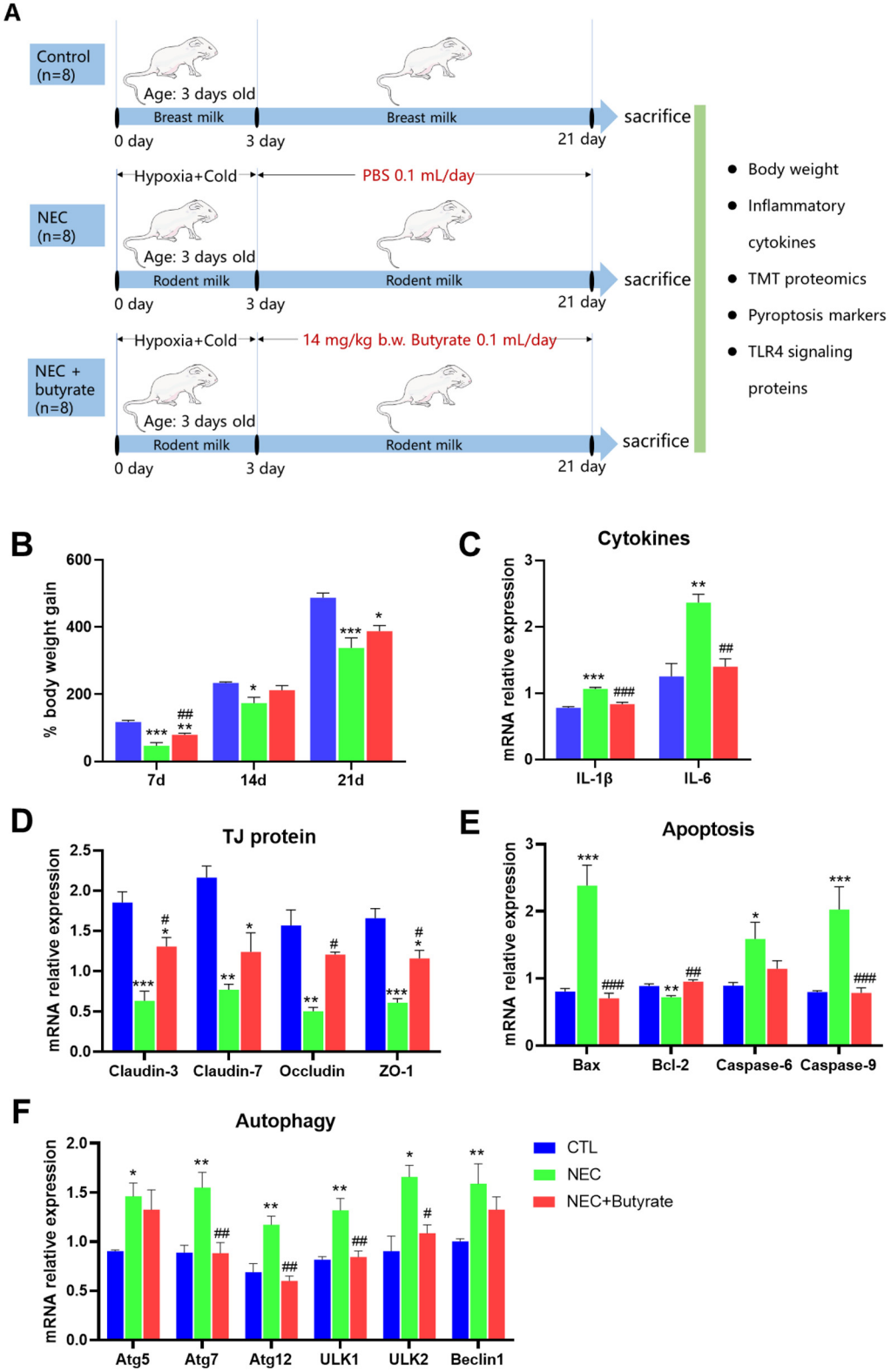

Fig. 1 Sodium butyrate (NaB) inhibited alleviated necrotizing enterocolitis-induced intestinal inflammation and disrupted intestinal barrier in neonatal rats. (A) The simplified flow chart of *in vivo* experiments. Neonatal rats were divided into the control, NEC, and butyrate + NEC groups. The simplified flow chart of *in vivo* experiments. (B) The measurement of body weight gain (%) on the 7th, 14th, and 21st days. (C) The mRNA expression levels of *IL-1β* and *IL-6* in the ileum. (D) The tight junction (TJ)-related mRNA relative expression, including *claudin-3*, *claudin-7*, *occludin*, and *ZO-1* in the ileum. (E) The apoptosis-related mRNA relative expression, including *Bax*, *Bcl-2*, *caspase-6*, and *caspase-9* in the ileum. (F) The autophagy-related mRNA relative expression, including *Atg5*, *Atg7*, *Atg12*, *ULK1*, *ULK2*, and *Beclin1* in the ileum. All the results are represented as mean ± SEM. *p < 0.05, **p < 0.01, and ***p < 0.001, *versus* the control group; $^{\#}$ p < 0.05, $^{\#\#}$ p < 0.01, and $^{\#\#\#}$ p < 0.001, *versus* the NEC rat group.

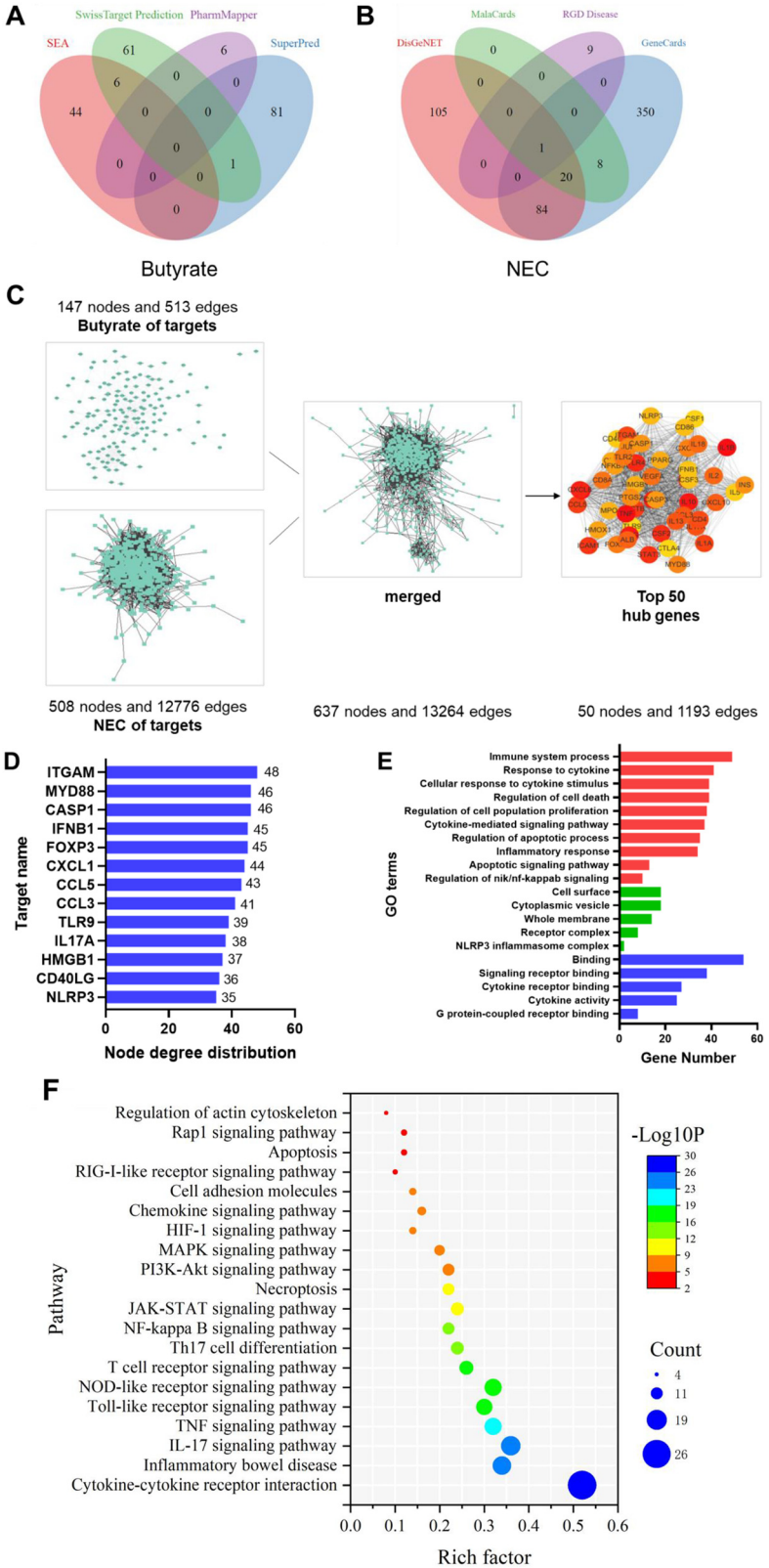

Fig. 2 The construction of network pharmacology for exploring sodium butyrate (NaB) activity against NEC. (A) Venn diagrams showing NaB and NEC targets obtained from five different databases. (B) The topology of core targets involved in the NaB activity against NEC. The color in nodes represents the degree number—the redder the color, the more the degree number. (C) The top targets with node degree >35. (D) The GO terms analysis of the top 50 hub genes, including terms of biological process (red), cellular component (green), and molecular function (blue). (E) The KEGG pathways enrichment of the top 50 hub genes. (F) The size of each dot indicates the corresponding number of genes. The color represents −log 10 (*p*-value).

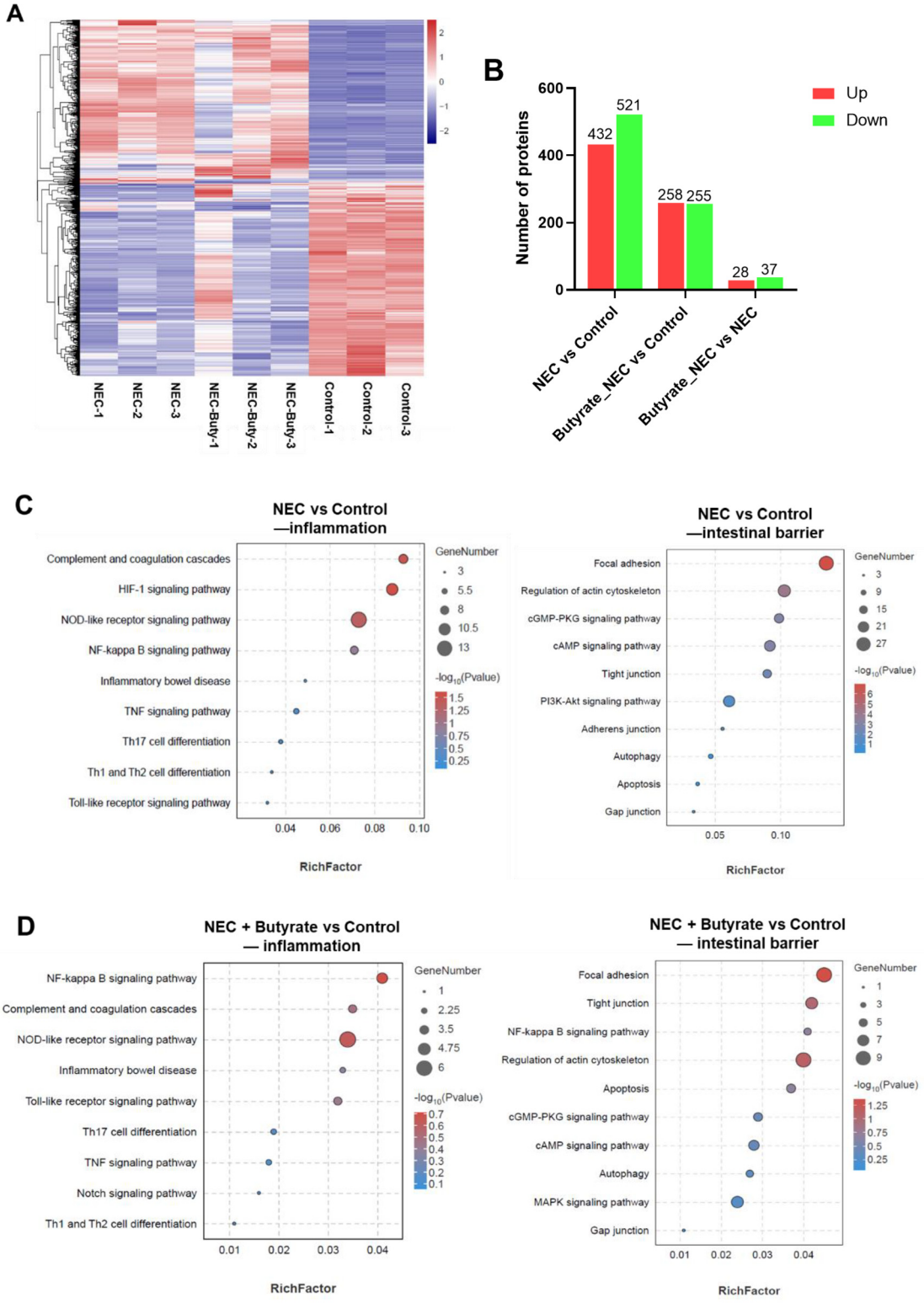

Fig. 3 The proteome analysis of sodium butyrate (NaB)-treated NEC neonatal rats. (A) Two-dimensional hierarchical clustering of protein expression profiles among control, NEC, and butyrate + NEC groups. (B) Histogram showing the number of up and down-regulated identified differentially expressed proteins in the different groups. (C–E) The inflammation and intestinal barrier-related KEGG pathways in the control, NEC, and butyrate + NEC groups. (F) The protein levels of pyroptosis markers (NLRP3 and GSDMD) and TLR4/MyD88/NF-κB signaling in the ileum. NaB reduced pyroptosis-induced intestinal inflammation and NF-κB signaling in NEC neonatal rats. All results are expressed as mean ± SEM. *$p < 0.05$, **$p < 0.01$, and ***$p < 0.001$ *versus* the control group; $^{\#}$ $p < 0.05$ and $^{\#\#}$ $p < 0.01$ *versus* the NEC group.

NEC-induced disruption of the neonatal intestinal barrier through cellular TJ proteins, cell apoptosis and autophagy. Furthermore, the enrichment analysis of the relevant pathways regulating intestinal inflammation and barrier indicated that the NF-κB signaling pathway played an important role in regulating the NEC after administration of NaB (Fig. 3C–E). These results were consistent with those from network pharmacology enrichment analysis.

Next, the results of the network pharmacology and proteomic analysis were verified using western blot assay. As shown in Fig. 2, the pharmacology network analysis showed that the NLRP3 inflammasome complex and NF-κB signaling pathway were involved in the anti-NEC effects of NaB. The genes encoding NLRP3, MyD88, and TLR4 were found to be the hub genes in this pharmacology network analysis. Additionally, the proteomics results indicated that the NF-κB signaling pathway played an important role in regulating the NEC of NaB, and the NLRP3 inflammasome complex was associated with the regulation of inflammation (Fig. 3C–E). Therefore, combining the results of pharmacology network analysis and proteomics analysis, the expression of NLRP3, GSDMD, TLR4, MyD88, and NF-κB was evaluated by western blot assay.

The results of the assay showed that, compared with the NEC group, NaB addition significantly decreased the protein levels of the indicators of NLRP3-dependent pyroptosis (NLRP3 and GSDMD) ($p < 0.05$, Fig. 3F). Additionally, NaB also significantly inhibited the protein levels of TLR4, MyD88, and NF-κB in neonatal rats with NEC ($p < 0.05$, Fig. 3F). These results were consistent with those of network pharmacology and proteomic analysis, demonstrating that NLRP3-dependent pyroptosis and the TLR4/MyD88/NF-κB pathway were essential for mediating the protective effects of NaB against NEC. As a result of these findings, the causal relationship between NLRP3-dependent pyroptosis and the TLR4-mediated NF-κB pathway were explored next.

3.4 Molecular docking analysis of potential targets

Molecular docking analysis was performed to elucidate a potential causal relationship between NaB-induced NLRP3-dependent pyroptosis and TLR4-mediated NF-κB signaling, which was confirmed by the network pharmacology and proteomic analysis. The molecular docking between the target proteins (including TLR4, MyD88, NF-κB, NLRP3, caspase-1, and GSDMD) and NaB were assessed *via* AutoDock software and the visual results were obtained in 2D and 3D modes. As shown in Fig. 4, among these target proteins, NaB interacted only with TLR4 (PBD ID: 3VQ1) and NF-κB (PBD ID: 1VKX). NaB was conjugated with TLR4 *via* two hydrogen bonds with different amino acids [LYS341 (1.86 Å) and LYS367 (3.69 Å)] (Fig. 4A, B and Table S5†). Furthermore, NaB was found to interact with LYS218 in NF-κB *via* one hydrogen bond [LYS218 (2.02 Å)] (Fig. 4C, D and Table S5†). The binding energies for TLR4 and NF-κB were −3.37 and −3.57 kcal mol^{-1} (Table S5†), suggesting the likelihood of their interaction with NaB. These results showed that NaB directly interacted with the TLR4-mediated NF-κB signaling pathway instead of NLRP3-dependent pyroptosis, indicating that NaB might inhibit NLRP3-dependent pyroptosis by restricting the TLR4/MyD88/NF-κB signaling pathway and, in turn, attenuating NEC.

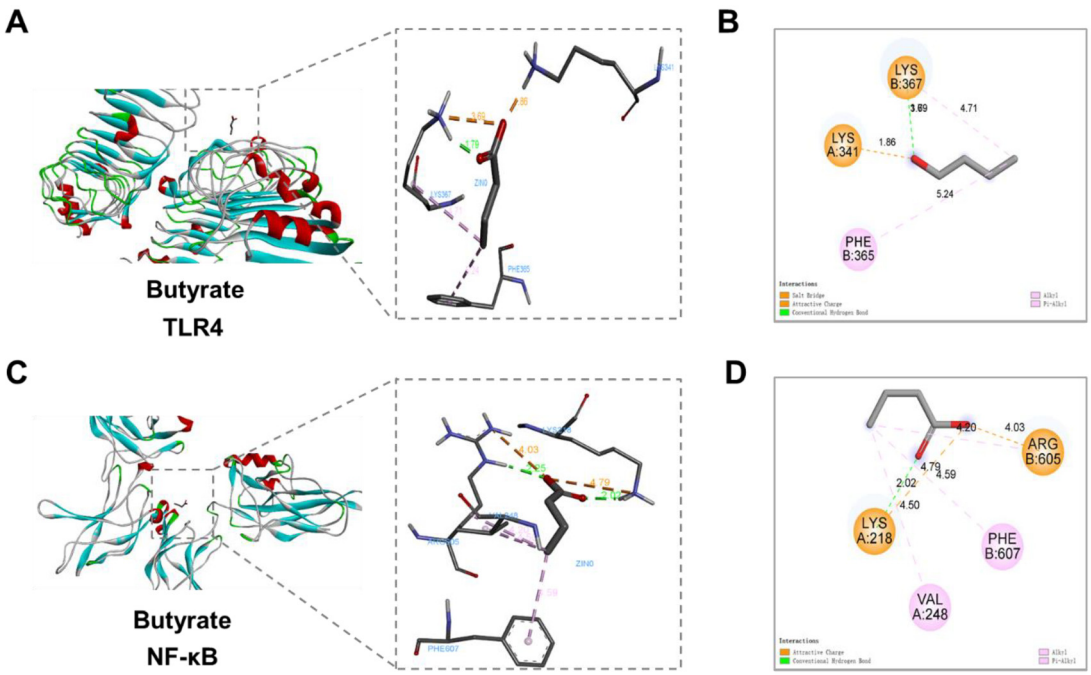

Fig. 4 Molecular docking model of sodium butyrate (NaB) with its potential targets. (A) 3D crystal structure docking model of TLR4 (PDBID: 3VQ1). (B) 2D docking model of TLR4. (C) 3D crystal structure docking model of NF-κB (PDBID: 1VKX). (D) 2D docking model of NF-κB.

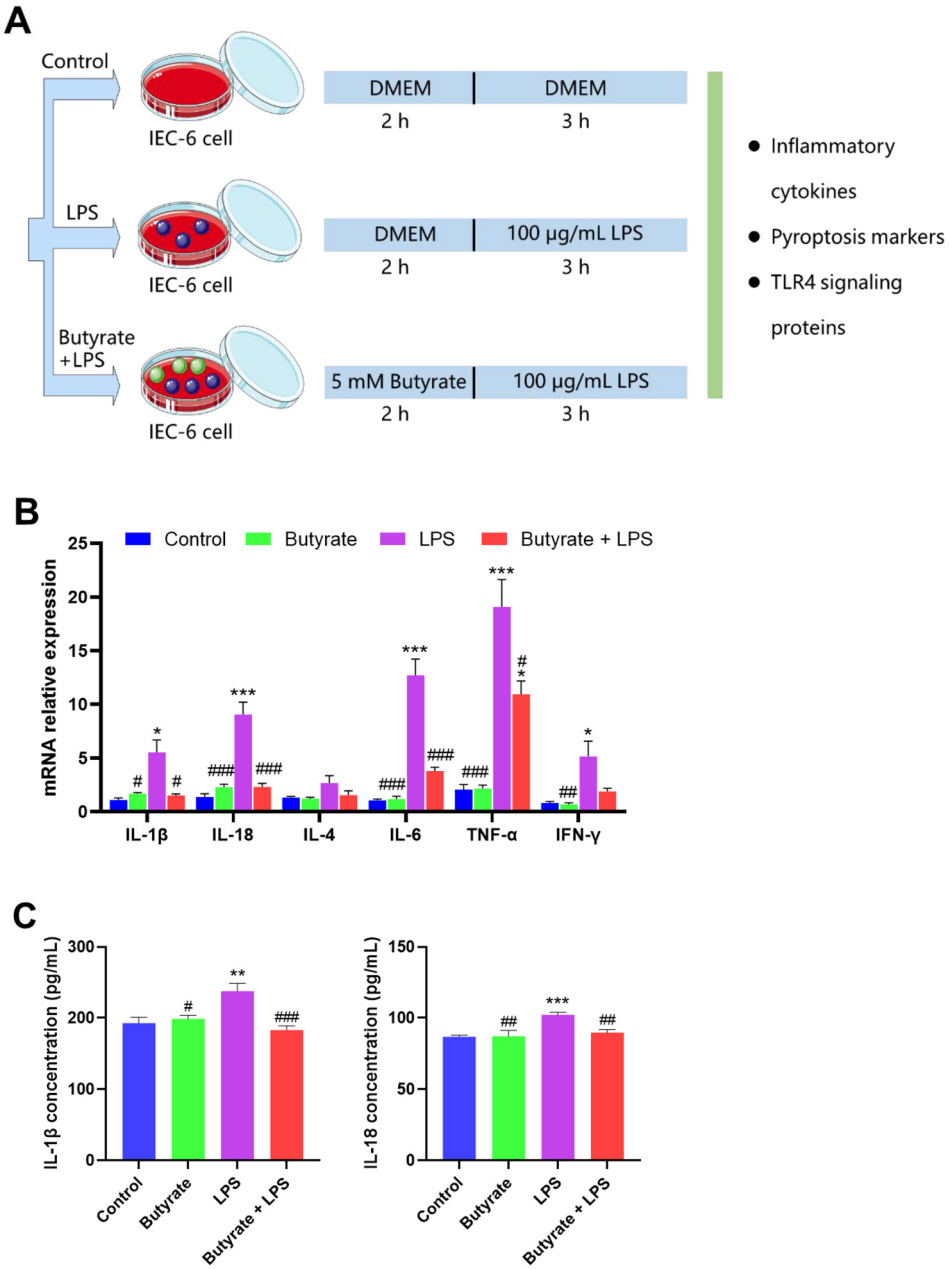

Fig. 5 Sodium butyrate (NaB) inhibited LPS-induced intestinal inflammation *in vitro*. (A) The simplified flow chart of *in vitro* experiments. IEC-6 cells were divided into the control, LPS, and butyrate + LPS groups. (B) The mRNA expression levels of the inflammatory factors obtained from the top 50 hub genes (including IL-1β, IL-18, IL-4, IL-6, TNF-α, and IFN-γ) in cells pretreated with 5 mM butyrate for 2 h and 100 μg mL^{-1} LPS for 3 h. (C) The secretion of inflammatory factors IL-1β and IL-18 quantified by ELISA in cells pretreated with 5 mM butyrate for 2 h and 100 μg mL^{-1} LPS for 3 h. (D) The mRNA levels of pyroptosis- and NF-κB-related genes (including TLR4, MyD88, NF-κB, NLRP3, caspase-1, and GSDMD) in cells pretreated with 5 mM butyrate for 2 h and 100 μg mL^{-1} LPS for 3 h. (E) The protein levels of pyroptosis- and NF-κB-related proteins in cells pretreated with 5 mM butyrate for 2 h and 100 μg mL^{-1} LPS for 3 h. All results are expressed as mean ± SEM. *$p < 0.05$, **$p < 0.01$, and ***$p < 0.001$ *versus* the control group; $^{\#}p < 0.05$, $^{\#\#}p < 0.01$, and $^{\#\#\#}p < 0.001$ *versus* the LPS group.

3.5 Inhibition of *in vitro* LPS-induced intestinal inflammation by NaB

To validate the molecular docking results, the effects of NaB against an LPS-induced *in vitro* NEC model was used (Fig. 5A). RT-qPCR results showed that the mRNA levels of inflammatory cytokines (*IL-1β*, *IL-18*, *IL-4*, *IL-6*, *TNF-α*, and *IFN-γ*) selected from the hub genes significantly increased post-LPS stimulation ($p < 0.05$). However, NaB treatment significantly reversed the upregulation of these genes ($p < 0.05$, Fig. 5B). Moreover, among these inflammatory cytokines, compared with the LPS group, NaB decreased the secretion of the pyroptosis markers (IL-1β and IL-18, Fig. 5C). In addition, the results of RT-qPCR and western blot assay demonstrated that NaB significantly

reversed the LPS-induced increase in the mRNA and protein levels of TLR4, MyD88, NF-κB, NLRP3, cleaved caspase-1, and GSDMD, respectively ($p < 0.05$, Fig. 5D and E). These findings were consistent with those of the *in vivo* assay, indicating that the NaB-induced alleviation of inflammatory responses in IEC-6 cells was mediated *via* NLRP3-mediated pyroptosis and TLR4-mediated NF-κB signaling.

3.6 Suppression of *in vitro* LPS-induced intestinal inflammation *via* the NaB-mediated modification of NLRP3-dependent pyroptosis

Firstly, to explore the potential relationship between TLR4-mediated NF-κB signaling and NLRP3-mediated pyroptosis, IEC-6 cells were treated with TAK-242, a TLR4 inhibitor (Fig. 6A). The western blot assay results showed that compared with the LPS group, TAK-242 treatment significantly reduced the protein expression of several TLR4/MyD88/NF-κB signaling pathway components and NLRP3-related pyroptosis ($p < 0.05$, Fig. 6B). These findings indicated that the TLR4-mediated NF-κB pathway might regulate NLRP3-dependent pyroptosis.

To further explore the underlying relationship between inflammatory responses and NLRP3-mediated pyroptosis, IEC-6 cells were treated with MCC950, an NLRP3 inhibitor (Fig. 7A). MCC950 pretreatment significantly reduced the protein levels of NLRP3, cleaved caspase-1, and GSDMD and the mRNA levels of IL-1β, IL-18, IL-4, IL-6, TNF-α, and IFN-γ ($p < 0.05$, Fig. 7B and C). These findings suggested that NLRP3-dependent pyroptosis might regulate the inflammatory responses. The results of inhibitors (TAK-242 and MCC950) were consistent with the effects of NaB treatment both *in vivo* and *in vitro*, indicating that NaB attenuated NEC *via* suppression of NLRP3-dependent pyroptosis and that the TLR4/MyD88/NF-κB signaling pathway is essential for NaB activity.

4. Discussion

NEC represents a major and fatal intestinal disorder found in premature infants, therefore, novel preventive and treatment strategies for NEC are urgently required. As the primary metabolite present in breast milk, butyrate has been reported to mediate its preventive effects against NEC. However, the fundamental processes underlying NaB-mediated protection are still unknown. In the present study, we firstly used rat pups with NEC to demonstrate a protective effect of NaB against NEC and the intestinal barrier *in vivo*. We then used network pharmacology and proteome analysis to screen vital targets and pathways, which were further validated *via* molecular docking and inhibitor assay *in vitro*.

From this, we demonstrated that NaB can protect immature intestinal function through enhancing the expression of TJ proteins and decreasing apoptosis and autophagy. These results were consistent with our recent reported study, showing that the integrity of the intestinal villi can be restored with the addition of NaB.[26] It has been reported that NaB can reverse the disrupted intestinal barrier induced by inflammation and that mRNA expression levels of TJ proteins (*occludin*, *claudin-2*, *claudin-5*, and *ZO-1*) in the colon of Western-style diet-fed C7BL/6 mice was significantly increased by the addition of NaB.[27] In weanling piglets, NaB significantly reduced the apoptotic cell number and the mRNA expression of *caspase-3* in the jejunum induced by LPS.[28] Furthermore, it has been reported that compared to healthy control groups, ulcerative colitis patients were observed with a greater number of autophagosomes, and that this autophagy could be suppressed by NaB as well as reduced in HT29 cells.[29]

The results of pharmacology networks and functional validations *in vivo* and *in vitro* showed that NaB-mediated NEC alleviation is mediated *via* NLRP3-dependent pyroptosis. Previous studies have reported that pyroptosis is a form of programmed cell death (PCD), known as "caspase 1-dependent PCD", which is pivotal in innate immunity.[30] NLRP3 is an inflammasome sensor. Once activated, it interacts with caspase-1, which, in turn, converts pro-IL-1β and pro-IL-18 into their biologically active forms.[31] At the same time, activated caspase-1 converts GSDMD into GSDMD-N with the cleaved N-terminal domain, leading to increased cell permeability resulting in the release of IL-1β and IL-18 from the cells, thereby inducing an inflammatory response.[32]

Pyroptosis-induced inflammation can be found in various vital organs of the body, including the gastrointestinal tract. Therefore, pyroptosis might play a part in the development of inflammatory bowel disease (IBD).[33] Although it has been reported that pyroptosis performs a double-sided effect in IBD development, many studies have demonstrated that the inhibition of pyroptosis might ameliorate the severity of IBD in mice. Caspase-1 inhibition has been reported to exert protective effects in a DSS-induced colitis experimental model.[34] Furthermore, the severity of DSS-induced colitis was reportedly attenuated by IL-18 neutralization.[34] Moreover, a recent study demonstrated enhanced pyroptosis in the intestine of exacerbated IBD patients.[35] Another study on MODE-K cells and a mouse model showed that the knockout of NEK7, a component of the NLRP3 inflammasome, significantly ameliorated chronic colitis.[36] In addition, a reduction in the expression of pyroptosis-related proteins, including NLRP3, led to protective effects in experimental colitis mouse models.[37,38]

Compared to the control samples, NLRP3 expression was increased in samples from children with NEC. Additionally, elevated secretion of IL-1β, IL-6, and TNF-α was also detected in their serum.[39] Immunohistochemistry results showed that the increased frequency of NLRP3 and caspase-1 positive cells was found in the intestinal-tissue segments collected from NEC infants.[40] Recent studies of mice with NEC and cell models have demonstrated that the NLRP3/caspase-1/IL-1β signaling pathway may be the underlying mechanism responsible for the development of NEC, and related therapeutic targets of these could be developed to alleviate the intestinal inflammation and injury seen with NEC.[5,41,42] Melatonin has been reported to attenuate the severity of NEC by repressing the acti-

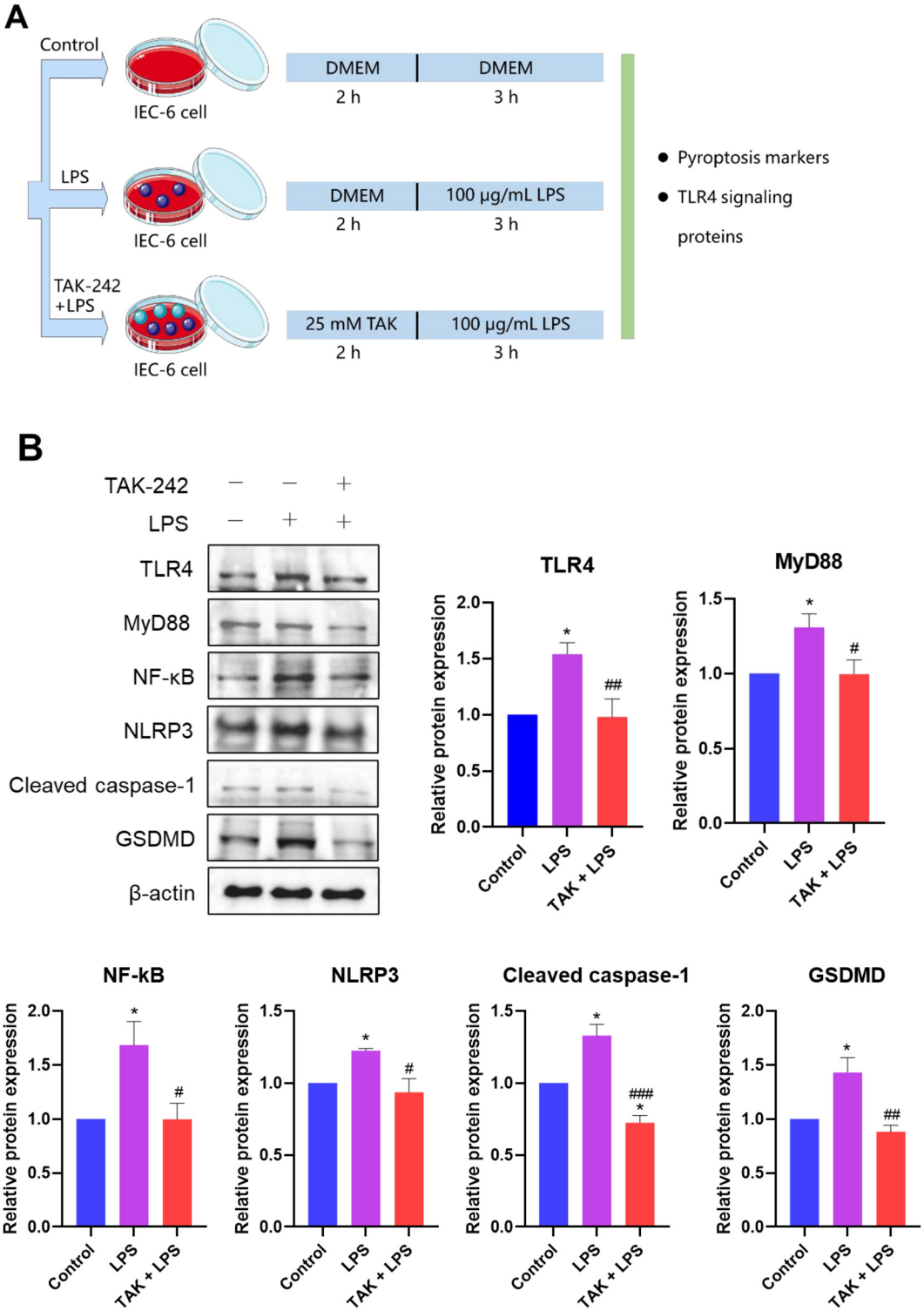

Fig. 6 Sodium butyrate (NaB) prevented NLRP3-dependent pyroptosis by inhibiting the TLR4/MyD88/NF-κB signaling pathway *in vitro*. (A) The simplified flow chart of *in vitro* experiments. IEC-6 cells were divided into the control, LPS, and TAK-242 + LPS groups. (B) The protein expressions of TLR4, MyD88, NF-κB, NLRP3, cleaved caspase-1, and GSDMD induced by LPS as well as TAK-242 and LPS treatment. All results are expressed as mean ± SEM. *$p < 0.05$, **$p < 0.01$, and ***$p < 0.001$ *versus* the control group; $^{\#}p < 0.05$, $^{\#\#}p < 0.01$, and $^{\#\#\#}p < 0.001$ *versus* the LPS group.

vation of the NLRP3 inflammasome.[43] Clinical samples, NEC rat models, and *in vitro* experiments have revealed that *Bacteroides fragilis* alleviated NEC through inhibiting the NLRP3 signaling pathway.[44] These findings were consistent with the results of the current study, showing that NaB alleviates NEC by inhibiting NLRP3-dependent pyroptosis.

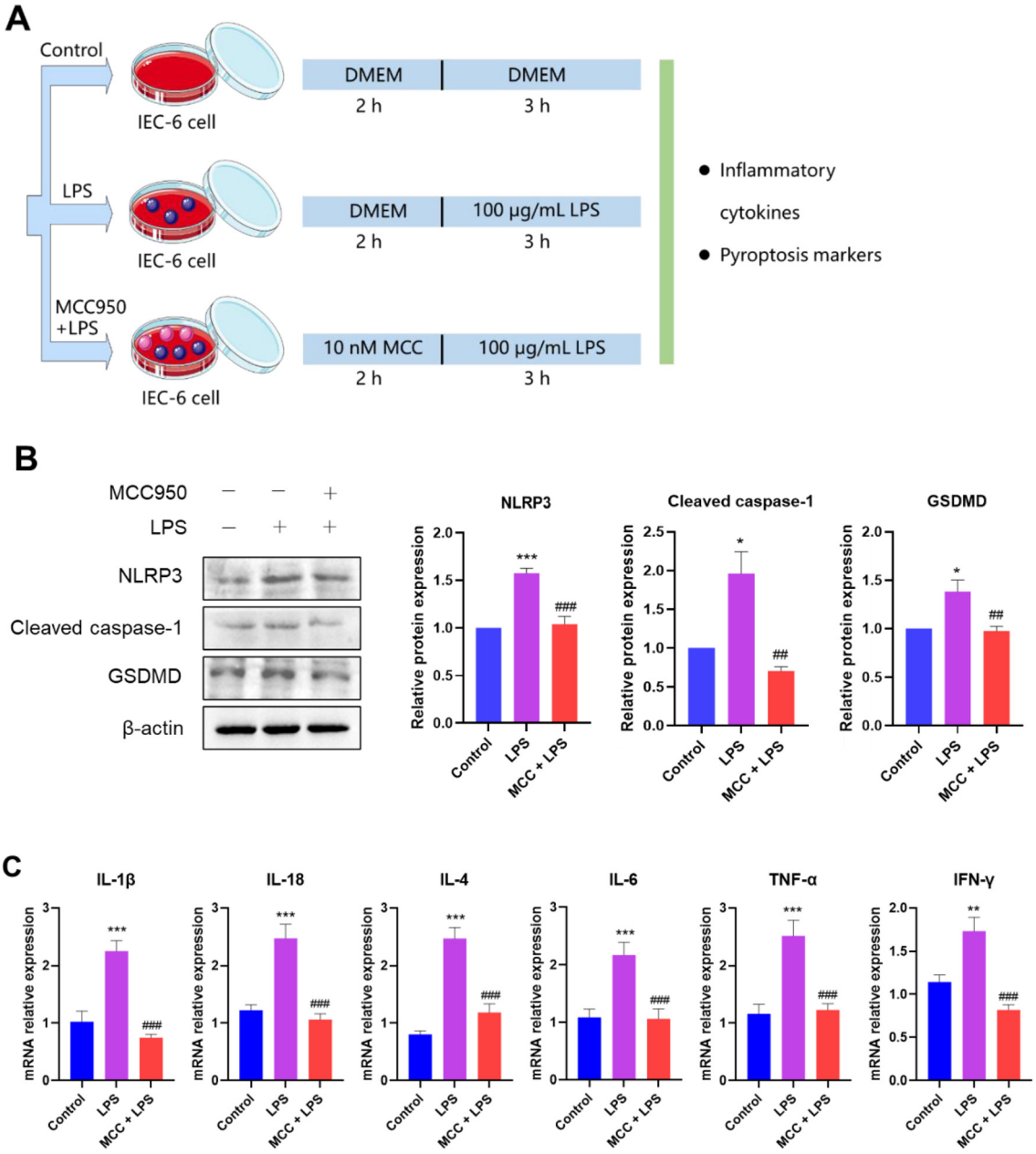

Fig. 7 Sodium butyrate (NaB) inhibited LPS-induced intestinal inflammation *via* NLRP3-dependent pyroptosis in IEC-6 cells. (A) The simplified flow chart of *in vitro* experiments. IEC-6 cells were divided into the control, LPS, and MCC950 + LPS groups. (B) The protein levels of NLRP3, cleaved caspase-1, and GSDMD in cells induced by MCC950 and LPS. (C) The mRNA levels of inflammatory cytokines in cells induced by MCC950 and LPS. All results are expressed as mean ± SEM. *$p < 0.05$, **$p < 0.01$, and ***$p < 0.001$ *versus* the control group; $^{\#}p < 0.05$, $^{\#\#}p < 0.01$, and $^{\#\#\#}p < 0.001$ *versus* the LPS group.

It has previously been demonstrated that diverse exogenous stimuli could activate the NLRP3 inflammasome; however, it is unlikely for NLRP3 to bind directly to these ligands. Therefore, the specific activation mechanism of the NLRP3 inflammasome needs to be further explored.[31] In the present study, functional validation *in vitro* revealed that NaB inhibited NLRP3-dependent pyroptosis by suppressing the TLR4/MyD88/NF-κB signaling pathway, thus exerting an anti-NEC effect. Previous studies have reported that the Nrf2/HO-1, MAPK, and NF-κB signaling pathways are upstream regulators of pyroptosis.[45,46] Human and mouse experiments have shown that the inhibition of NLRP3-induced pyroptosis was mediated by the suppression of NF-κB signaling.[47] In addition, TLR4 is considered an important regulator of the canonical NLRP3 inflammasome pathway.[48] In H9C2 cells, doxorubicin has been shown to initiate the formation of TLR4 and NLRP3 inflammasomes, inducing pyroptosis.[49] These findings demonstrated that TLR4-dependent NF-κB signaling is necess-

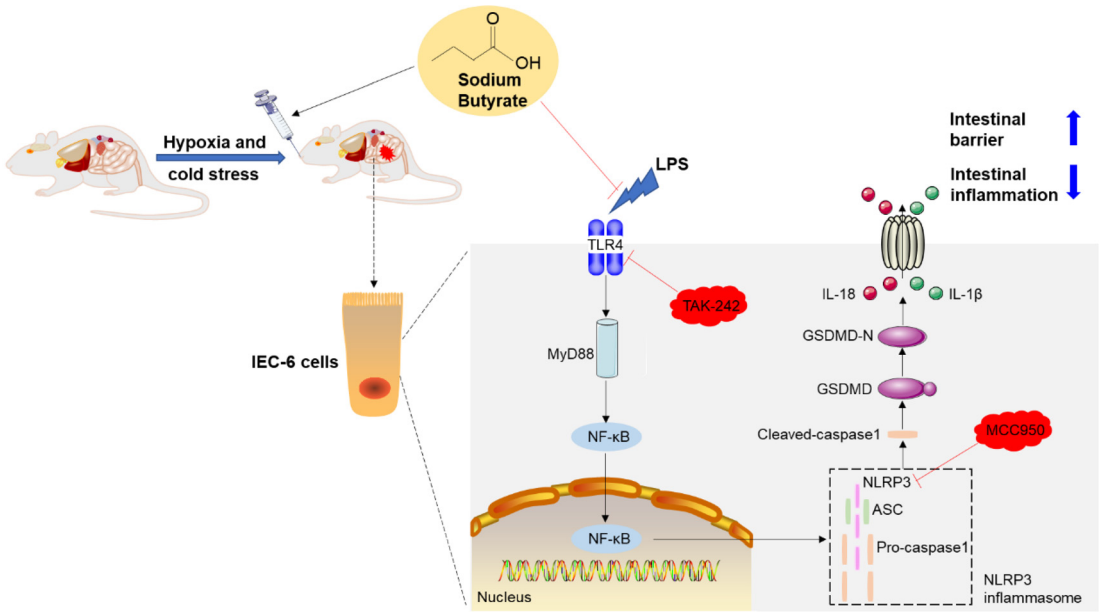

Fig. 8 Schematic mechanism underlying NaB activity against NEC *in vivo* and *in vitro*. NaB attenuated NEC by inhibiting NLRP3-dependent pyroptosis, partially by suppressing the TLR4/MyD88/NF-κB signaling pathway.

ary to activate pyroptosis. In addition, both cell and chronic colitis mouse models have shown that LPS activates the NLRP3 inflammasome *via* the TLR4/NF-κB pathway.[36,50] TAK-242 treatment in mice and human kidney cells revealed that the inhibition of TLR4/NF-κB signaling led to suppressed pyroptosis, and ameliorated the secretion of inflammatory cytokines (IL-1β and IL-18).[51]

Studies of the small intestine from patients with NEC and mouse models have found that the expression of TLR4 significantly increased.[52,53] The importance of intestinal TLR4 in the pathogenesis of NEC has been revealed by studies showing that in mice deficient in TLR4 at the intestinal epithelium the development of NEC could be inhibited.[54] It has been reported that milk fat globule membrane ameliorated NEC *in vivo* and *in vitro* through suppressing inflammation *via* the TLR4/MyD88/NF-κB pathway.[23] Additionally, the *in vitro* NEC model established with IEC-6 cells showed that the TLR4/NF-κB pathway was involved in the pathogenesis of NEC.[55]

Although a few studies have shown that NaB regulates NLRP3-mediated pyroptosis through TLR4-meditated NF-κB signaling, various substances have been demonstrated to perform such a function. In HTR-8/SVneo cells, metformin partially alleviated NLRP3-mediated pyroptosis by suppressing TLR4/NF-κB signaling.[56] The hepatoprotective effect of octreotide in rats was associated with a decrease in pyroptosis mediated *via* the inhibition of the TLR4/NF-κB/NLRP3 signaling pathway.[57] Nicorandil reduced NLRP3 inflammasome-mediated pyroptosis by suppressing TLR4/MyD88/NF-κB signaling, thus protecting the rats against myocardial infarction.[58] In addition, *in vivo* and *in vitro* experiments have demonstrated that salidroside ameliorates Parkinson's disease by suppressing NLRP3-dependent pyroptosis, partly by inhibiting TLR4/MyD88/NF-κB signaling.[59] In addition, it has been reported that the increased expression of TJ proteins induced by kaempferol and maresin 1 in animal models of DSS-induced ulcerative colitis was associated with the TLR4/NF-κB signaling pathway.[60,61] Furthermore, baicalin significantly decreased apoptosis-related proteins in ulcerative colitis through NF-κB signaling.[62] It has been reported that the inhibition of NLRP3 *via* the TLR4 and NF-κB signaling pathways were involved in the improvement of NEC.[63] Furthermore, curcumin may improve NEC-induced cell pyroptosis (NLRP3 and caspase-1 expression) by inhibiting the TLR4 signaling pathway in newborn rats.[64] The suppressor of cytokine signaling 3 protected against NEC *via* suppressing the NLRP3 inflammasome in a TLR4 dependent manner.[65] The protective effects of sialylated human milk oligosaccharides on NEC may be due to the suppression of TLR4/NF-κB/NLRP3-mediated inflammation.[56] In the present study, as shown in Fig. 8, NaB was found to attenuate NEC by suppressing NLRP3 inflammasome-dependent pyroptosis *via* TLR4-mediated modulation of NF-κB signaling.

5. Conclusions

In our study, we firstly confirmed that NaB exerts an intestinal protective effect on NEC *in vivo*, and then used network pharmacology to predict the potential targets of NaB associated with NEC. The results of network pharmacology were verified by *in vivo* experiments and proteomics. The results showed that NLRP3-dependent pyroptosis and TLR4-mediated NF-κB signaling were involved in the anti-NEC effect of NaB. Furthermore, preliminary validation of molecular docking and

in vitro NEC modeling, combined with inhibitor assays involving TAK-242 and MCC950, demonstrated that NaB ameliorated NEC by inhibiting NLRP3-dependent pyroptosis *via* suppression of TLR4/MyD88/NF-κB signaling (Fig. 8). These findings suggest that inhibition of NLRP3-dependent pyroptosis or NaB supplementation might be used as a novel preventive and treatment strategy for NEC.

Author contributions

Yanan Gao: conceptualization, methodology, formal analysis, investigation, writing – original draft & review & editing, visualization. Liting Yang: methodology, validation. Hongya Wu: validation. Qianqian Yao: writing – review & editing. Jiaqi Wang: supervision, conceptualization. Nan Zheng: funding acquisition, resources.

Data availability

The original contributions presented in the study are included in the article/ESI,† further inquiries can be directed to the corresponding author.

Conflicts of interest

All the authors declare no conflict of interest.

Acknowledgements

This study was supported by the National Key R&D Program of China (2022YFD1600104), the earmarked fund for CARS (CARS-36), the Agricultural Science and Technology Innovation Program (ASTIP-IAS12).

References

1 D. F. Nino, C. P. Sodhi and D. J. Hackam, Necrotizing enterocolitis: new insights into pathogenesis and mechanisms, *Nat. Rev. Gastroenterol. Hepatol.*, 2016, **13**(10), 590–600, DOI: **10.1038/nrgastro.2016.119**.

2 J. Neu and W. A. Walker, Medical Progress: Necrotizing Enterocolitis, *N. Engl. J. Med.*, 2011, **364**(3), 255–264, DOI: **10.1056/NEJMra1005408**.

3 L. P. Chen, Z. B. Lv, Z. M. Gao, G. J. Ge, X. L. Wang, J. M. Zhou and Q. F. Sheng, Human β-defensin-3 reduces excessive autophagy in intestinal epithelial cells and in experimental necrotizing enterocolitis, *Sci. Rep.*, 2019, **9**, 19890, DOI: **10.1038/s41598-019-56535-3**.

4 Y. J. Yang, T. Zhang, G. Y. Zhou, X. X. Jiang, M. X. Tao, J. X. Zhang, X. Q. Zeng, Z. Wu, D. D. Pan and Y. X. Guo, Prevention of necrotizing enterocolitis through milk polar lipids reducing intestinal epithelial apoptosis, *J. Agric. Food Chem.*, 2020, **68**, 7014–7023, DOI: **10.1021/acs.jafc.0c02629**.

5 Y. Zhang, O. Wang, H. Y. Mi, J. J. Yi and S. B. Cai, Rhus chinensis Mill. fruits prevent necrotizing enterocolitis in rat pups via regulating the expressions of key proteins involved in multiple signaling pathways, *J. Ethnopharmacol.*, 2022, **290**, 115103, DOI: **10.1016/j.jep.2022.115103**.

6 B. Shi, C. J. Lyu, Z. K. Le, H. S. Ji, Y. Xiao, Y. Y. Zhang, S. J. Huang, L. J. Yu, Q. Shu, J. F. Tou and D. M. Lai, NLRP3 activation in macrophages promotes acute intestinal injury in neonatal necrotizing enterocolitis, *World J. Pediatr.*, 2024, **20**(2), 153–164, DOI: **10.1007/s12519-023-00727-5**.

7 A. L. Meister, K. K. Doheny and R. A. Travagli, Necrotizing enterocolitis: It's not all in the gut, *Exp. Biol. Med.*, 2020, **245**(2), 85–95, DOI: **10.1177/1535370219891971**.

8 D. L. O'Connor, S. Gibbins, A. Kiss, N. Bando, J. Brennan-Donnan, E. Ng, D. M. Campbell, S. Vaz, C. Fusch, E. Asztalos, P. Church, E. Kelly, L. Ly, A. Daneman, S. Unger and GTA DoMINO Feeding Group, Effect of Supplemental Donor Human Milk Compared With Preterm Formula on Neurodevelopment of Very Low-Birth-Weight Infants at 18 Months A Randomized Clinical Trial, *JAMA, J. Am. Med. Assoc.*, 2016, **316**(18), 1897–1905, DOI: **10.1001/jama.2016.16144**.

9 W. A. Walker and R. S. Iyengar, Breast milk, microbiota, and intestinal immune homeostasis, *Pediatr. Res.*, 2015, **77**(1), 220–228, DOI: **10.1038/pr.2014.160**.

10 W. A. Walker and D. Meng, *Breast Milk and Microbiota in the Premature Gut: A Method of Preventing Necrotizing Enterocolitis*, 4th Nestle-Nutrition-Institute Workshop, Karger, Lausanne, Switzerland, 2019, pp. 103–112.

11 L. F. Stinson, M. C. L. Gay, P. T. Koleva, M. Eggesb, C. C. Johnson, G. Wegienka, E. du Toit, N. Shimojo, D. Munblit, D. E. Campbell, S. L. Prescott, D. T. Geddes and A. L. Kozyrskyj, Human Milk From Atopic Mothers Has Lower Levels of Short Chain Fatty Acids, *Front. Immunol.*, 2020, **11**, 9, DOI: **10.3389/fimmu.2020.01427**.

12 F. Teng, P. Wang, L. Yang, Y. Ma and L. Day, Quantification of Fatty Acids in Human, Cow, Buffalo, Goat, Yak, and Camel Milk Using an Improved One-Step GC-FID Method, *Food Anal. Methods*, 2017, **10**(8), 2881–2891, DOI: **10.1007/s12161-017-0852-z**.

13 J. M. Pestana, A. Gennari, B. W. Monteiro, D. N. Lehn and C. F. V. Souza, Effects of Pasteurization and Ultra-High Temperature Processes on Proximate Composition and Fatty Acid Profile in Bovine Milk, *Am. J. Food Technol.*, 2015, **10**(6), 265–272, DOI: **10.3923/ajft.2015.265.272**.

14 Y. He, W. X. Du, S. Xiao, B. H. Zeng, X. She, D. Liu, H. Du, L. Q. Li, F. Li, Q. Ai, J. L. He, C. Song, H. Wei, X. D. Zhao and J. L. Yu, Colonization of fecal microbiota from patients with neonatal necrotizing enterocolitis exacerbates intestinal injury in germfree mice subjected to necrotizing enterocolitis-induction protocol via alterations in butyrate and regulatory T cells, *J. Transl. Med.*, 2021, **19**(1), 12, DOI: **10.1186/s12967-021-03109-5**.

15 J. Liu, H. T. Zhu, B. Li, C. Lee, M. Alganabi, S. Zheng and A. Pierro, Beneficial effects of butyrate in intestinal injury,

J. Pediatr. Surg., 2020, **55**(6), 1088–1093, DOI: **10.1016/j.jpedsurg.2020.02.036**.

16 Y. N. Gao, B. Davis, W. S. Zhu, N. Zheng, D. Meng and W. A. Walker, Short-chain fatty acid butyrate, a breast milk metabolite, enhances immature intestinal barrier function genes in response to inflammation in vitro and in vivo, *Am. J. Physiol.: Gastrointest. Liver Physiol.*, 2021, **320**(4), G521–G530, DOI: **10.1152/ajpgi.00279.2020**.

17 S. N. Huang, Y. A. Gao, Z. W. Wang, X. Yang, J. Q. Wang and N. Zheng, Anti-inflammatory actions of acetate, propionate, and butyrate in fetal mouse jejunum cultures ex vivo and immature small intestinal cells in vitro, *Food Sci. Nutr.*, 2022, **10**(2), 564–576, DOI: **10.1002/fsn3.2682**.

18 B. Clancy, R. B. Darlington and B. L. Finlay, Translating developmental time across mammalian species, *Neuroscience*, 2001, **105**, 7–17, DOI: **10.1016/s0306-4522(01)00171-3**.

19 W. Y. Jiao, S. Mi, Y. X. Sang, Q. X. Jin, B. Chitrakar, X. H. Wang and S. Wang, Integrated network pharmacology and cellular assay for the investigation of an anti-obesity effect of 6-shogaol, *Food Chem.*, 2022, **374**(9), 131755, DOI: **10.1016/j.foodchem.2021.131755**.

20 M. Wolski, Modification of experimental model of necrotizing enterocolitis (nec) in rat pups by single exposure to hypothermia and hypoxia and impact of mother's milk on incidence of disease, *Med. Sci. Monit.*, 2024, **30**, e943443, DOI: **10.12659/MSM.943443**.

21 Q. S. Xie, J. X. Zhang, M. Liu, P. H. Liu, Z. J. Wang, L. Zhu, L. Jiang, M. M. Jin, X. N. Liu, L. Liu and X. D. Liu, Short-chain fatty acids exert opposite effects on the expression and function of p-glycoprotein and breast cancer resistance protein in rat intestine, *Acta Pharmacol. Sin.*, 2021, **42**(3), 470–481, DOI: **10.1038/s41401-020-0402-x**.

22 C. H. Chin, S. H. Chen, H. H. Wu, C. W. Ho, M. T. Ko and C. Y. Lin, cytoHubba: identifying hub objects and sub-networks from complex interactome, *BMC Syst. Biol.*, 2014, **8**, 7, DOI: **10.1186/1752-0509-8-s4-s11**.

23 D. Zhang, J. Wen, J. Zhou, W. Cai and L. Qian, Milk Fat Globule Membrane Ameliorates Necrotizing Enterocolitis in Neonatal Rats and Suppresses Lipopolysaccharide-Induced Inflammatory Response in IEC-6 Enterocytes, *JPEN, J. Parenter. Enteral Nutr.*, 2019, **43**, 863–873, DOI: **10.1002/jpen.1496**.

24 M. Good, R. H. Siggers, C. P. Sodhi, A. Afrazi, F. Alkhudari, C. E. Egan, M. D. Neal, I. Yazji, H. Jia, J. Lin, *et al.* Amniotic fluid inhibits Toll-like receptor 4 signaling in the fetal and neonatal intestinal epithelium, *Proc. Natl. Acad. Sci. U. S. A.*, 2012, **109**(28), 11330–11335, DOI: **10.1073/pnas.1200856109M**.

25 Y. Yuan, D. Ding, N. Zhang, Z. Xia, J. Wang, H. Yang, F. Guo and B. Li, TNF-α induces autophagy through ERK1/2 pathway to regulate apoptosis in neonatal necrotizing enterocolitis model cells IEC-6, *Cell Cycle*, 2018, **17**(11), 1390–1402, DOI: **10.1080/15384101.2018.1482150**.

26 Y. N. Gao, L. T. Yang, Q. Q. Yao, J. Q. Wang and N. Zheng, Butyrate improves recovery from experimental necrotizing enterocolitis by metabolite hesperetin through potential inhibition the PI3K-Akt pathway, *Biomed. Pharmacother.*, 2024, **176**, 116876, DOI: **10.1016/j.biopha.2024.116876**.

27 J. Beisner, L. Filipe Rosa, V. Kaden-Volynets, I. Stolzer, C. Günther and S. C. Bischoff, Prebiotic inulin and sodium butyrate attenuate obesity-induced intestinal barrier dysfunction by induction of antimicrobial peptides, *Front. Immunol.*, 2021, **12**, 678360, DOI: **10.3389/fimmu.2021.678360**.

28 Y. Han, C. Tang, Q. Zhao, S. Fan, P. Yang and J. Zhang, Butyrate mitigates lipopolysaccharide-induced intestinal morphological changes inweanling piglets by regulating the microbiota and energy metabolism, and alleviating inflammation and apoptosis, *Microorganisms*, 2022, **10**, 2001, DOI: **10.3390/microorganisms10102001**.

29 F. Zhang, W. Wang, J. Niu, G. Yang, J. Luo, D. Lan, J. Wu, M. Li, Y. Sun, K. Wang and Y. Miao, Heat-shock transcription factor 2 promotes sodium butyrate-induced autophagy by inhibiting mTOR in ulcerative colitis, *Exp. Cell Res.*, 2020, **388**(1), 111820, DOI: **10.1016/j.yexcr.2020.111820**.

30 L. Galluzzi, I. Vitale, S. A. Aaronson, J. M. Abrams, D. Adam, P. Agostinis, E. S. Alnemri, L. Altucci, I. Amelio, D. W. Andrews, M. Annicchiarico-Petruzzelli, A. V. Antonov, E. Arama, E. H. Baehrecke, N. A. Barlev, N. G. Bazan, *et al.*, Molecular mechanisms of cell death: recommendations of the Nomenclature Committee on Cell Death 2018, *Cell Death Differ.*, 2018, **25**(3), 486–541, DOI: **10.1038/s41418-017-0012-4**.

31 M. Zheng and T. D. Kanneganti, The regulation of the ZBP1-NLRP3 inflammasome and its implications in pyroptosis, apoptosis, and necroptosis (PANoptosis), *Immunol. Rev.*, 2020, **297**(1), 26–38, DOI: **10.1111/imr.12909**.

32 F. M. Jie, S. T. Xiao, Y. Qiao, Y. H. You, Y. Feng, Y. Long, S. X. Li, Y. L. Wu, Y. W. Li and Q. Du, Kuijieling decoction suppresses NLRP3-Mediated pyroptosis to alleviate inflammation and experimental colitis in vivo and in vitro, *J. Ethnopharmacol.*, 2021, **264**(12), 113243, DOI: **10.1016/j.jep.2020.113243**.

33 Y. A. Wei, L. Yang, A. Pandeya, J. Cui, Y. Zhang and Z. Y. Li, Pyroptosis-Induced Inflammation and Tissue Damage, *J. Mol. Biol.*, 2022, **434**(26), 167301, DOI: **10.1016/j.jmb.2021.167301**.

34 B. Siegmund, H. A. Lehr, G. Fantuzzi and C. A. Dinarello, IL-1 beta-converting enzyme (caspase-1) in intestinal inflammation, *Proc. Natl. Acad. Sci. U. S. A.*, 2001, **98**(23), 13249–13254, DOI: **10.1073/pnas.231473998**.

35 Z. H. Xu, R. T. Liu, L. Huang, Y. X. Xu, M. M. Su, J. Y. Chen, L. L. Geng, W. F. Xu and S. T. Gong, CD147 Aggravated Inflammatory Bowel Disease by Triggering NF-kappa B-Mediated Pyroptosis, *BioMed Res. Int.*, 2020, **2020**(8), 5341247, DOI: **10.1155/2020/5341247**.

36 X. Chen, G. Liu, Y. Yuan, G. Wu, S. Wang and L. Yuan, NEK7 interacts with NLRP3 to modulate the pyroptosis in inflammatory bowel disease via NF-kappaB signaling, *Cell Death Dis.*, 2019, **10**(12), 906, DOI: **10.1038/s41419-019-2157-1**.

37 L. M. Chao, Z. Q. Li, J. H. Zhou, W. Q. Chen, Y. F. Li, W. J. Lv, A. O. Guo, Q. Qu and S. N. Guo, Shen-Ling-Bai-Zhu-San Improves Dextran Sodium Sulfate-Induced Colitis by Inhibiting Caspase-1/Caspase-11-Mediated Pyroptosis, *Front. Pharmacol.*, 2020, **11**(10), 814, DOI: **10.3389/fphar.2020.00814**.

38 V. Neudecker, M. Haneklaus, O. Jensen, L. Khailova, J. C. Masterson, H. Tye, K. Biette, P. Jedlicka, K. S. Brodsky, M. E. Gerich, M. Mack, A. A. B. Robertson, M. A. Cooper, G. T. Furuta, C. A. Dinarello, L. A. O'Neill, H. K. Eltzschig, S. L. Masters and E. N. McNamee, Myeloid-derived miR-223 regulates intestinal inflammation via repression of the NLRP3 inflammasome, *J. Exp. Med.*, 2017, **214**(6), 1737–1752, DOI: **10.1084/jem.20160462**.

39 Q. Li, X. Lei, H. Liu, S. Feng, C. Cai, Y. Hu, Y. Cao and J. Chen, Transient receptor potential melastatin 7 aggravates necrotizing enterocolitis by promoting an inflammatory response in children, *Transl. Pediatr.*, 2022, **11**(12), 2030–2039, DOI: **10.21037/tp-22-633**.

40 W. Zhang, J. He-Yang, W. Tu and X. Zhou, Sialylated human milk oligosaccharides prevent intestinal inflammation by inhibiting toll like receptor 4/NLRP3 inflammasome pathway in necrotizing enterocolitis rats, *Nutr. Metab.*, 2021, **18**(1), 5, DOI: **10.1186/s12986-020-00534-z**.

41 L. Shen, X. Zhong, H. Ji, S. Yang, J. Jin, C. Lyu, Y. Ren, Y. Xiao, Y. Zhang, S. Fang, N. Lin, J. Tou, Q. Shu and D. Lai, Macrophage α7nAChR alleviates the inflammation of neonatal necrotizing enterocolitis through mTOR/NLRP3/IL-1β pathway, *Int. Immunopharmacol.*, 2024, **139**, 112590, DOI: **10.1016/j.intimp.2024.112590**.

42 X. Yang, X. Li, C. Wu and F. Zhang, Knockdown of PHLDA1 Alleviates Necrotizing Enterocolitis by Inhibiting NLRP3 Inflammasome Activation and Pyroptosis Through Enhancing Nrf2 Signaling, *Immunol. Invest.*, 2023, **52**(3), 257–269, DOI: **10.1080/08820139.2022.2161910**.

43 X. Xiong, Z. Bao, Y. Mi, X. Wang and J. Zhu, Melatonin Alleviates Neonatal Necrotizing Enterocolitis by Repressing the Activation of the NLRP3 Inflammasome, *Gastroenterol. Res. Pract.*, 2022, **2022**, 6920577, DOI: **10.1155/2022/6920577**.

44 Z. Chen, H. Chen, W. Huang, X. Guo, L. Yu, J. Shan, X. Deng, J. Liu, W. Li, W. Shen and H. Fan, Bacteroides fragilis alleviates necrotizing enterocolitis through restoring bile acid metabolism balance using bile salt hydrolase and inhibiting FXR-NLRP3 signaling pathway, *Gut Microbes*, 2024, **16**(1), 2379566, DOI: **10.1080/19490976.2024.2379566**.

45 C. C. Huang, C. T. Zhang, P. P. Yang, R. Chao, Z. Q. Yue, C. S. Li, J. Guo and M. Q. Li, Eldecalcitol Inhibits LPS-Induced NLRP3 Inflammasome-Dependent Pyroptosis in Human Gingival Fibroblasts by Activating the Nrf2/HO-1 Signaling Pathway, *Drug Des., Dev. Ther.*, 2020, **14**, 4901–4913, DOI: **10.2147/dddt.S269223**.

46 X. Li, Y. Zou, Y. Y. Fu, J. Xing, K. Y. Wang, P. Z. Wan, M. Wang and X. Y. Zhai, Ibudilast Attenuates Folic Acid-Induced Acute Kidney Injury by Blocking Pyroptosis Through TLR4-Mediated NF-kappaB and MAPK Signaling Pathways, *Front. Pharmacol.*, 2021, **12**, 650283, DOI: **10.3389/fphar.2021.650283**.

47 Y. Li, W. Song, Y. Tong, X. Zhang, J. Zhao, X. Gao, J. Yong and H. Wang, Isoliquiritin ameliorates depression by suppressing NLRP3-mediated pyroptosis via miRNA-27a/SYK/NF-kappaB axis, *J. Neuroinflammation*, 2021, **18**(1), 1, DOI: **10.1186/s12974-020-02040-8**.

48 M. Kinra, M. Nampoothiri, D. Arora and J. Mudgal, Reviewing the importance of TLR-NLRP3-pyroptosis pathway and mechanism of experimental NLRP3 inflammasome inhibitors, *Scand. J. Immunol.*, 2022, **95**(2), e13124, DOI: **10.1111/sji.13124**.

49 Z. T. Dargani and D. K. Singla, Embryonic stem cell-derived exosomes inhibit doxorubicin-induced TLR4-NLRP3-mediated cell death-pyroptosis, *Am. J. Physiol.: Heart Circ. Physiol.*, 2019, **317**(2), H460–H471, DOI: **10.1152/ajpheart.00056.2019**.

50 X. H. Liu, L. M. Wu, J. L. Wang, X. H. Dong, S. C. Zhang, X. H. Li, H. Xu, D. B. Liu, Z. H. Li, Z. M. Liu, S. G. Wu and Y. W. Hu, Long non-coding RNA RP11-490M8.1 inhibits lipopolysaccharide-induced pyroptosis of human umbilical vein endothelial cells via the TLR4/NF-kappaB pathway, *Immunobiology*, 2021, **226**(5), 152133, DOI: **10.1016/j.imbio.2021.152133**.

51 Y. Wang, X. Zhu, S. Yuan, S. Wen, X. Liu, C. Wang, Z. Qu, J. Li, H. Liu, L. Sun and F. Liu, TLR4/NF-kappaB Signaling Induces GSDMD-Related Pyroptosis in Tubular Cells in Diabetic Kidney Disease, *Front. Endocrinol.*, 2019, **10**, 603, DOI: **10.3389/fendo.2019.00603**.

52 Y. Yang, T. Zhang, G. Zhou, X. Jiang, M. Tao, J. Zhang, X. Zeng, Z. Wu, D. Pan and Y. Guo, Prevention of Necrotizing Enterocolitis through Milk Polar Lipids Reducing Intestinal Epithelial Apoptosis, *J. Agric. Food Chem.*, 2020, **68**(26), 7014–7023, DOI: **10.1021/acs.jafc.0c02629**.

53 Y. Jing, F. Peng, Y. Shan and J. Jiang, Berberine reduces the occurrence of neonatal necrotizing enterocolitis by reducing the inflammatory response, *Exp. Ther. Med.*, 2018, **16**(6), 5280–5285, DOI: **10.3892/etm.2018.6871**.

54 C. L. Leaphart, J. Cavallo, S. C. Gribar, S. Cetin, J. Li, M. F. Branca, T. D. Dubowski, C. P. Sodhi and D. J. Hackam, A critical role for TLR4 in the pathogenesis of necrotizing enterocolitis by modulating intestinal injury and repair, *J. Immunol.*, 2007, **179**(7), 4808–4820, DOI: **10.4049/jimmunol.179.7.4808**.

55 L. An, J. Li, B. Liu, J. Hui, Q. Zhang, X. Zhang and Q. Wang, Knockdown of TRPM7 attenuates apoptosis and inflammation in neonatal necrotizing enterocolitis model cell IEC-6 via modulating TLR4/NF-κB and MEK/ERK pathways, *Iran. J. Basic Med. Sci.*, 2022, **25**, 947–953, DOI: **10.22038/IJBMS.2022.62113.13742**.

56 Y. Zhang, W. Liu, Y. Zhong, Q. Li, M. Wu, L. Yang, X. Liu and L. Zou, Metformin Corrects Glucose Metabolism Reprogramming and NLRP3 Inflammasome-Induced Pyroptosis via Inhibiting the TLR4/NF-kappaB/PFKFB3

Signaling in Trophoblasts: Implication for a Potential Therapy of Preeclampsia, *Oxid. Med. Cell. Longevity*, 2021, **2021**, 1806344, DOI: **10.1155/2021/1806344**.

57 A. E. E. El-Sisi, S. S. Sokar, A. M. Shebl, D. Z. Mohamed and S. E. Abu-Risha, Octreotide and melatonin alleviate inflammasome-induced pyroptosis through inhibition of TLR4-NF-kappaB-NLRP3 pathway in hepatic ischemia/reperfusion injury, *Toxicol. Appl. Pharmacol.*, 2021, **410**, 115340, DOI: **10.1016/j.taap.2020.115340**.

58 F. Chen, Z. Q. Chen, G. L. Zhong and J. J. Zhu, Nicorandil inhibits TLR4/MyD88/NF-kappaB/NLRP3 signaling pathway to reduce pyroptosis in rats with myocardial infarction, *Exp. Biol. Med.*, 2021, **246**(17), 1938–1947, DOI: **10.1177/15353702211013444**.

59 X. Zhang, Y. M. Zhang, R. Li, L. P. Zhu, B. Q. Fu and T. H. Yan, Salidroside ameliorates Parkinson's disease by inhibiting NLRP3-dependent pyroptosis, *Aging*, 2020, **12**(10), 9405–9426, DOI: **10.18632/aging.103215**.

60 S. Qiu, P. Li, H. Zhao and X. Li, Maresin 1 alleviates dextran sulfate sodium-induced ulcerative colitis by regulating NRF2 and TLR4/NF-kB signaling pathway, *Int. Immunopharmacol.*, 2020, **78**, 106018, DOI: **10.1016/j.intimp.2019.106018**.

61 Y. Qu, X. Li, F. Xu, S. Zhao, X. Wu, Y. Wang and J. Xie, Kaempferol alleviates murine experimental colitis by restoring gut microbiota and inhibiting the LPS-TLR4-NF-kB axis, *Front. Immunol.*, 2021, **12**, 679897, DOI: **10.3389/fimmu.2021.679897**.

62 J. Shen, J. Cheng, S. Zhu, J. Zhao, Q. Ye, Y. Xu, H. Dong and X. Zheng, Regulating effect of baicalin on IKK/IKB/NF-kB signaling pathway and apoptosis-related proteins in rats with ulcerative colitis, *Int. Immunopharmacol.*, 2019, **73**, 193–200, DOI: **10.1016/j.intimp.2019.04.052**.

63 R. Yu, S. Jiang, Y. Tao, P. Li, J. Yin and Q. Zhou, Inhibition of HMGB1 improves necrotizing enterocolitis by inhibiting NLRP3 via TLR4 and NF-κB signaling pathways, *J. Cell. Physiol.*, 2019, **234**(8), 13431–13438, DOI: **10.1002/jcp.28022**.

64 Y. Yin, X. Wu, B. Peng, H. Zou, S. Li, J. Wang and J. Cao, Curcumin improves necrotising microscopic colitis and cell pyroptosis by activating SIRT1/NRF2 and inhibiting the TLR4 signalling pathway in newborn rats, *Innate Immun.*, 2020, **26**(7), 609–617, DOI: **10.1177/1753425920933656**.

65 H. Zhang, Y. Wang, S. Li, X. Tang, R. Liang and X. Yang, SOCS3 protects against neonatal necrotizing enterocolitis via suppressing NLRP3 and AIM2 inflammasome activation and p65 nuclear translocation, *Mol. Immunol.*, 2020, **122**, 21–27, DOI: **10.1016/j.molimm.2020.03.019**.